Chuchard et al. *Advances in Difference Equations* (2017) 2017:160
DOI 10.1186/s13662-017-1209-z

Advances in Difference Equations
a SpringerOpen Journal

RESEARCH Open Access

Study of pulsatile pressure-driven electroosmotic flows through an elliptic cylindrical microchannel with the Navier slip condition

Pearanat Chuchard[1], Somsak Orankitjaroen[1,2*] and Benchawan Wiwatanapataphee[3]

*Correspondence:
somsak.ora@mahidol.ac.th
[1]Department of Mathematics, Faculty of Science, Mahidol University, Rama VI Road, Bangkok, 10400, Thailand
[2]The Centre of Excellence in Mathematics, Si Ayutthaya Road, Bangkok 10400, Thailand
Full list of author information is available at the end of the article

Abstract

This paper aims to study an unsteady electric field-driven and pulsatile pressure-driven flow of a Newtonian fluid in an elliptic cylindrical microchannel with Navier boundary wall slip. The governing equations of the slip flow and distributions of electric potential and charge densities are the modified Navier-Stokes equations, the Poisson equation and the Nernst-Planck equations, respectively. Analytical and numerical analyses based on the Mathieu and modified Mathieu equations are performed to investigate the interplaying effects of pulsatile pressure gradients and the slip lengths on the electroosmotic flow.

Keywords: microchannel flow; elliptic cross-section; Navier-Stokes equations; pulsatile pressure gradient; elctroosmosis; electric potential

1 Introduction

Over the past decades, a fluid flow manipulation under a very small scale known as microfluidics has become an active field of scientific research due to the emergence of their several applications, for example, lab-on-the-chips, computer chips, medical diagnostic devices, and drug delivery systems [1–5]. Taking the advantage of a small scale system, a microfluidic application not only reduces the requirement for the samples, but also increases the efficiency and speed of the reaction. As a consequence, the microflow characteristics have been widely studied in both experimental and analytical ways in order to develop various system controls and device designs [6–10]. One particular technique to precisely manipulate a flow in a microscale is the use of a pressure force combined with the well-known electrokinetic force, namely, electroosmosis. Electroosmosis phenomenon relies on the formation of the electrical double layer (EDL) generated by two parallel layers of charged ions: the first layer, the layer of ions on the inner wall surface due to the chemical reaction between the fluid and the channel wall; the second layer, the layer of counter ions in the fluid attracted to the first layer by the Coulomb force. The movement of the ions in the second layer, induced by the application of an external electric field, will lead to the motion of the entire fluid caused by the drag force [11].

Fluid flow problems have been carried out traditionally under the no-slip boundary condition [12–14], which dictates that the velocity, relative to the wall channel, of the fluid adjacent to the wall is zero. However, in microfluidics, the appearance of the fluid slip at the wall interface has been widely reported, and its influence has been investigated [15–17]. For this reason, the velocity slip condition turns into an important factor to achieve the realistic microflow behavior.

In the literature, an analytic solution of an electroosmotic flow in microchannels has been studied under a constant pressure gradient. Goswami and Chakraborty [10] investigated the semi-analytic solution of a steady electroosmotic flow with the interfacial slip condition in microchannels of various complex cross-sectional shapes under the constant pressure gradient assumption. Na *et al*. [18], Chinyoka and Makinde [19], and Reshad *et al*. [20] found the analytic solution of transient electroosmotic and pressure-driven flows with a constant pressure gradient through a microannulus, a slip microchannel, and rectangular microchannels, respectively. However, some microfluidic systems are driven by a pulsatile pressure gradient due to the nature of some systems such as blood flow or the integrated micropump of displacement type. Moreover, a report of Bandopadhyay and Chakraborty [21] on the investigation of electroosmotic flow in a slip microchannel shows that the overestimation result can be obtained under the avoidance of a pulsating pressure gradient. As a result, a microfluidic investigation combined with a pulsating pressure gradient is a key to keeping the problem suitable in many situations. Recently, the solution of combined pulsating pressure gradient and electroosmotic flow was found by Chakraborty *et al*. [22], but the pressure gradient was simplified to just a sinusoidal function.

Due to the fact that the geometry in many microfluidic devices and some systems such as a blood vessel is of a circular or elliptic cross-section, the use of elliptic geometry takes an advantage of embodying the solution for circular geometry and making the problem tractable for any eccentricity.

According to the aforementioned arguments, we here derive the solution of combined pulsatile pressure-driven and electroosmotic flow through an elliptic cylindrical microchannel under the Navier slip condition to describe the flow behavior in a more realistic situation than the previous works. The pressure gradient term in Navier-Stokes equations is precisely expanded by the Fourier series. Moreover, an influence of a pulsatile pressure gradient, the number of the Fourier expansion terms for the pressure gradient, and a slip length are investigated on the volumetric flow rate which plays a more important role in the flow control in microfluidic devices compared to the velocity profile.

2 Preliminaries

In this section, we introduce the elliptic cylindrical coordinates, the Mathieu and modified Mathieu functions which are used throughout this paper.

2.1 Elliptic cylindrical coordinate system

Considering an elliptic cylindrical geometry having two foci on x-axis at $x = \pm c$ of the Cartesian coordinate system (x, y, z), we define the elliptic cylindrical coordinates (ξ, η, z) by

$$x = c\cosh\xi\cos\eta, \qquad y = c\sinh\xi\sin\eta, \quad \text{and} \quad z = z,$$

where $0 \leq \xi < \infty$, $0 \leq \eta < 2\pi$, and $-\infty < z < \infty$. The coordinates ξ and η respectively correspond to the confocal elliptic cylinder and the asymptotic angle of the confocal hyperbolic cylinder with the identities

$$\frac{x^2}{c^2\cosh^2\xi} + \frac{y^2}{c^2\sinh^2\xi} = 1 \quad \text{and} \quad \frac{x^2}{c^2\cos^2\eta} - \frac{y^2}{c^2\sin^2\eta} = 1.$$

The scale factors are

$$h_\xi = h_\eta = c\sqrt{\cosh^2\xi - \cos^2\eta} \quad \text{and} \quad h_z = 1,$$

and the Laplacian is

$$\nabla^2 = \frac{1}{c^2(\cosh^2\xi - \cos^2\eta)}\left(\frac{\partial^2}{\partial\xi^2} + \frac{\partial^2}{\partial\eta^2}\right) + \frac{\partial^2}{\partial z^2}.$$

2.2 Mathieu functions

The solutions of the 2-dimensional wave equation in the elliptical coordinates,

$$\frac{1}{c^2(\cosh^2\xi - \cos^2\eta)}\left(\frac{\partial^2 W}{\partial\xi^2} + \frac{\partial^2 W}{\partial\eta^2}\right) + k^2 W = 0, \tag{1}$$

were introduced by the French mathematician, Émile Léonard Mathieu, in 1868 as the eigensolutions of the Mathieu differential equations to determine the motion of an elliptic stretched membrane [23]. The method splits equation (1) into two ordinary differential equations with the separation constant a as follows:

$$\frac{d^2G}{d\eta^2} + (a - 2q\cos 2\eta)G = 0, \tag{2}$$

$$\frac{d^2F}{d\xi^2} - (a - 2q\cosh 2\xi)F = 0, \tag{3}$$

where $q = k^2c^2/4 > 0$. Equations (2) and (3) are respectively named the Mathieu and modified Mathieu equations, and their solutions corresponding to special values of the separation constant (characteristic numbers) are called the Mathieu and modified Mathieu functions. These characteristic numbers are the functions of q. Hence, the solutions of equation (1), in an elliptic geometry, can be written as a linear combination of the periodic Mathieu functions of η and the modified Mathieu functions of ξ:

$$\begin{aligned} W(\xi,\eta) = \sum_{m=1}^{\infty}\big[&C_{1m}\,\mathrm{Ce}_m(\xi,q)\,\mathrm{ce}_m(\eta,q) + C_{2m}\,\mathrm{Fe}_m(\xi,q)\,\mathrm{ce}_m(\eta,q) \\ &+ S_{1m}\,\mathrm{Se}_m(\xi,q)\,\mathrm{se}_m(\eta,q) + S_{2m}\,\mathrm{Ge}_m(\xi,q)\,\mathrm{se}_m(\eta,q)\big], \end{aligned} \tag{4}$$

where $\mathrm{ce}_m(\eta,q)$, $\mathrm{se}_m(\eta,q)$ are the periodic Mathieu functions; $\mathrm{Ce}_m(\eta,q)$, $\mathrm{Se}_m(\eta,q)$ are the periodic modified Mathieu functions; and $\mathrm{Fe}_m(\eta,q)$, $\mathrm{Ge}_m(\eta,q)$ are the non-periodic modified Mathieu functions. The formulas of Mathieu and modified Mathieu equations can be found in [24].

3 Mathematical modeling

In this section, we construct the fundamental equation of the problem. The governing equations of a transient electroosmotic flow for an incompressible Newtonian fluid through an elliptical tube, with the z-axis being the channel-length direction, are the continuity equation and the incompressible Navier-Stokes equations as given below:

$$\nabla \cdot \mathbf{v} = 0, \tag{5}$$

$$\rho\left(\frac{\partial \mathbf{v}}{\partial t} + (\mathbf{v} \cdot \nabla)\mathbf{v}\right) = -\nabla p + \mu \nabla^2 \mathbf{v} + \mathbf{F}_{\mathrm{ek}}, \tag{6}$$

where $\mathbf{v} = (v_\xi, v_\eta, v_z)$ and ρ are respectively the velocity and the density of fluid, p is the pressure, and μ is the viscosity. The electrokinetic body force $\mathbf{F}_{\mathrm{ek}}$ is defined by $\mathbf{F}_{\mathrm{ek}} = \rho_e \mathbf{E}$, where $\mathbf{E}$ is the external electric field and ρ_e is the ionic charge density given by the Poisson equation

$$\nabla^2 \psi(\xi, \eta) = -\frac{\rho_e}{\varepsilon}, \tag{7}$$

where ε is the permittivity of the fluid and ψ is the potential inside the channel. In this study, we focus on a fully developed flow along the z-axial direction, *i.e.*, $\mathbf{v} = (0, 0, v_z)$, $\nabla p = (0, 0, \partial p/\partial z)$, $\mathbf{E} = (0, 0, E)$. Then the continuity equation (5) now becomes $\partial v_z/\partial z = 0$, which gives rise to $v_z = u(\xi, \eta, t)$, and the incompressible Navier-Stokes equations (6) can be reduced to the form

$$\nabla^2\left(u - \frac{\varepsilon E}{\mu}\psi\right) - \frac{\rho}{\mu}\frac{\partial u}{\partial t} = \frac{1}{\mu}\frac{\partial p}{\partial z}, \tag{8}$$

where $\partial p/\partial z$ depends only on t. Letting $U = u - (\varepsilon E \mu^{-1})\psi$, we express equation (8) as

$$\frac{1}{c^2(\cosh^2 \xi - \cos^2 \eta)}\left(\frac{\partial^2 U}{\partial \xi^2} + \frac{\partial^2 U}{\partial \eta^2}\right) - \frac{\rho}{\mu}\frac{\partial U}{\partial t} = \frac{1}{\mu}\frac{\partial p}{\partial z}. \tag{9}$$

As mentioned before, in this study, we consider a time periodic function of the pressure gradient driving the flow. To be precise, $\partial p/\partial z$ is time periodic and can be expressed by

$$\frac{\partial p}{\partial z}(t) = a_0 + \sum_{n=1}^{\infty}\left[a_n \cos(n\omega t) + b_n \sin(n\omega t)\right] = \mathrm{Re}\left(\sum_{n=0}^{\infty} c_n \mathrm{e}^{in\omega t}\right), \tag{10}$$

where the complex constants c_n are defined by $c_0 = a_0$ and $c_n = a_n - b_n i$, a_n, b_n are real, and ω is the frequency. As equation (9) is linear, we can use the superposition principle for the solution, *i.e.*, if U_n is a solution of equation (9) for $\partial p/\partial z = c_n \exp(in\omega t)$, then the complete solution of equation (9) for $\partial p/\partial z = \mathrm{Re}(\sum_{n=0}^{\infty} c_n \exp(in\omega t))$ is $U = \sum_{n=0}^{\infty} \mathrm{Re}(U_n)$.

For the electrical double layer field acting only in the direction perpendicular to the boundary, the boundary conditions for the potential distribution ψ are as follows: (i) ψ is constant on the boundary and (ii) $\partial\psi/\partial n = 0$ at the center of the channel. Consider that fluid flow and the potential distribution are symmetric about x- and y-axes, the boundary conditions in elliptic cylindrical coordinates are given by

$$\frac{\partial u}{\partial \eta}(\xi, 0, t) = \frac{\partial \psi}{\partial \eta}(\xi, 0) = 0 \quad \text{implying that } \frac{\partial U}{\partial \eta}(\xi, 0, t) = 0, \tag{11a}$$

$$\frac{\partial u}{\partial \eta}\left(\xi, \frac{\pi}{2}, t\right) = \frac{\partial \psi}{\partial \eta}\left(\xi, \frac{\pi}{2}\right) = 0 \quad \text{implying that } \frac{\partial U}{\partial \eta}\left(\xi, \frac{\pi}{2}, t\right) = 0, \tag{11b}$$

$$\frac{\partial u}{\partial \xi}(0, \eta, t) = \frac{\partial \psi}{\partial \xi}(0, \eta) = 0 \quad \text{implying that } \frac{\partial U}{\partial \xi}(0, \eta, t) = 0, \tag{11c}$$

with the Navier slip condition of a non-movement channel

$$u(\xi_0, \eta, t) + \frac{l}{c\sqrt{\cosh^2 \xi_0 - \cos^2 \eta}} \frac{\partial u}{\partial \xi}(\xi_0, \eta, t) = 0, \tag{11d}$$

and the constant zeta potential ζ at the wall

$$\psi(\xi_0, \eta) = \zeta, \tag{11e}$$

where l is the slip length, $\xi_0 = \ln((1 + \sqrt{1 - \bar{e}^2})\bar{e}^{-1})$ is the boundary interface, and $\bar{e}$ is the eccentricity of the ellipse.

4 Solution of the boundary value problem

In this section, we construct the solution of transient combined pulsatile pressure-driven and electroosmotic flow for an incompressible Newtonian fluid through an elliptical tube. Hereafter, the symbol $'$ denotes the differentiation with respect to ξ. To determine the velocity $u(\xi, \eta, t)$, we solve

$$\frac{1}{c^2(\cosh^2 \xi - \cos^2 \eta)}\left(\frac{\partial^2 U_n}{\partial \xi^2} + \frac{\partial^2 U_n}{\partial \eta^2}\right) - \frac{\rho}{\mu}\frac{\partial U_n}{\partial t} = \frac{c_n}{\mu} e^{in\omega t}.$$

Letting $U_n = f_n \exp(in\omega t)$, where $f_n = f_n(\xi, \eta)$, we use the identities $\cosh^2 \xi = (1 + \cosh 2\xi)/2$ and $\cos^2 \eta = (1 + \cos 2\eta)/2$ to arrive at

$$\frac{2}{c^2(\cosh 2\xi - \cos 2\eta)}\left(\frac{\partial^2 f_n}{\partial \xi^2} + \frac{\partial^2 f_n}{\partial \eta^2}\right) - \frac{in\omega\rho}{\mu} f_n = \frac{c_n}{\mu}. \tag{12}$$

For constant pressure ($n = 0$), equation (12) becomes

$$\frac{\partial^2 f_0}{\partial \xi^2} + \frac{\partial^2 f_0}{\partial \eta^2} = \frac{c_0 c^2}{2\mu}(\cosh 2\xi - \cos 2\eta). \tag{13}$$

The non-homogeneous equation (13) can be solved by the eigenfunction expansion with the boundary conditions (11a)-(11c), and thus the solution f_0 is in the form

$$f_0(\xi, \eta) = A_0 + \sum_{m=1}^{\infty} A_{2m} \cosh(2m\xi)\cos(2m\eta) + \bar{c}_0(\cosh 2\xi + \cos 2\eta),$$

where A_{2m} are constants to be determined and $\bar{c}_0 = c_0 c^2 (8\mu)^{-1}$.

For the pulsatile pressure gradient ($n \geq 1$), we let $f_n = W_n(\xi, \eta) - \bar{c}_n$, where $\bar{c}_n = c_n(in\omega\rho)^{-1}$, and then write equation (12) for W_n as

$$\frac{2}{c^2(\cosh 2\xi - \cos 2\eta)}\left(\frac{\partial^2 W_n}{\partial \xi^2} + \frac{\partial^2 W_n}{\partial \eta^2}\right) - \frac{in\omega\rho}{\mu} W_n = 0. \tag{14}$$

Equation (14) is now in the form of the 2-dimensional wave equation in elliptic coordinates, and hence, the solutions W_n are in the form of the Mathieu and modified Mathieu equations as we mention in Section 2.2 for $q = -is_n = -in\omega\rho c^2\{4\mu\}^{-1}$. In this study, we assume that U is symmetrical about x- and y-axes. Since the symmetry is governed by the function of η and only $\mathrm{ce}_{2m}(\eta, q)$ are symmetrical about the both axes, the solutions in the form of equation (4) can be simplified to

$$W_n(\xi,\eta) = \sum_{m=0}^{\infty}\left[B_{2m}^n \mathrm{Ce}_{2m}(\xi,-is_n) + C_{2m}^n \mathrm{Fe}_{2m}(\xi,-is_n)\right]\mathrm{ce}_{2m}(\eta,-is_n),$$

where B_{2m}^n and C_{2m}^n are constant. Because $\mathrm{Fe}'_{2m}(0,-is_n) \neq 0$, the constants C_m^n must be zero to satisfy the boundary condition (11c). Hence, the solutions W_n can be reduced to

$$W_n(\xi,\eta) = \sum_{m=0}^{\infty} B_{2m}^n \mathrm{Ce}_{2m}(\xi,-is_n)\,\mathrm{ce}_{2m}(\eta,-is_n).$$

From the superposition principle, the flow velocity u is in the form

$$\begin{aligned} u(\xi,\eta) &= \frac{\varepsilon E}{\mu}\psi + \sum_{n=0}^{\infty}\mathrm{Re}(U_n) \\ &= \frac{\varepsilon E}{\mu}\psi + f_0 + \sum_{n=1}^{\infty}\mathrm{Re}\left([W_n - \bar{c}_n]e^{in\omega t}\right) \\ &= \frac{\varepsilon E}{\mu}\psi + \frac{A_0}{2} + \sum_{m=1}^{\infty} A_{2m}\cosh(2m\xi)\cos(2m\eta) + \bar{c}_0\left[\cosh(2\xi)+\cos(2\eta)\right] \\ &\quad + \sum_{n=1}^{\infty}\sum_{m=0}^{\infty}\mathrm{Re}\left(\left[B_{2m}^n \mathrm{Ce}_{2m}(\xi,-is_n)\,\mathrm{ce}_{2m}(\eta,-is_n) - \bar{c}_n\right]\mathrm{e}^{in\omega t}\right). \end{aligned} \tag{15}$$

To find constants A_{2m} and B_{2m}^n, we substitute u from equation (15) into the Navier slip boundary condition (11d) using the value of ψ in equation (11e). By equating the terms having the same exponential, we then have

$$\begin{aligned} 0 &= \frac{\varepsilon E}{\mu}\left[\zeta + g(\eta,l)\frac{\partial\psi}{\partial\xi}(\xi_0,\eta)\right] + \frac{A_0}{2} \\ &\quad + \sum_{m=1}^{\infty}\left[A_{2m}\left(\cosh(2m\xi_0) + 2mg(\eta,l)\sinh(2m\xi_0)\right)\cos(2m\eta)\right] \\ &\quad + \bar{c}_0\left[\cosh(2\xi_0)+\cos(2\eta)+2g(\eta,l)\sinh(2\xi_0)\right], \end{aligned} \tag{16}$$

and for $n \geq 1$,

$$0 = \sum_{m=0}^{\infty} B_{2m}^n\left[\mathrm{Ce}_{2m}(\xi_0,-is_n) + g(\eta,l)\,\mathrm{Ce}'_{2m}(\xi_0,-is_n)\right]\mathrm{ce}_{2m}(\eta,-is_n) - \bar{c}_n, \tag{17}$$

where $g(\eta,l) = lc^{-1}(\cosh^2\xi_0 - \cos^2\eta)^{-1/2}$. For $l = 0$, *i.e.*, $g(\eta,l) = 0$, the constants A_{2m} and B_{2m}^n can be derived by using the orthogonality of the trigonometric functions and the

Mathieu functions, respectively:

$$\begin{aligned} A_{2m} &= \frac{\int_0^{2\pi} [\varepsilon E\zeta/\mu + \bar{c}_0[\cosh(2\xi_0) + \cos(2\eta)]]\cos(2m\eta)\,d\eta}{\int_0^{2\pi} \cosh(2m\xi_0)\cos^2(2m\eta)\,d\eta}, \\ B_{2m}^n &= \frac{\int_0^{2\pi} \bar{c}_n \operatorname{ce}_{2m}(\eta, -is_n)\,d\eta}{\int_0^{2\pi} \operatorname{Ce}_{2m}(\xi_0, -is_n)\operatorname{ce}_{2m}^2(\eta, -is_n)\,d\eta}. \end{aligned} \tag{18}$$

For $l > 0$, let k be a non-negative integer. Multiplying equations (16) and (17) by $\cos(2k\eta)$ and $\operatorname{ce}_{2k}(\eta, -is_n)$ respectively and integrating from 0 to 2π with respect to η, we then have the following system of equations:

$$\sum_{m=0}^{\infty} M_{k,m}A_{2m} = N_k \quad \text{and} \quad \sum_{m=0}^{\infty} O_{k,m}^n B_{2m}^n = P_k^n, \tag{19}$$

where

$$\begin{aligned} M_{k,m} &= \int_0^{2\pi} \big[\cosh(2m\xi_0) + g(\eta, l)2m\sinh(2m\xi_0)\big]\cos(2m\eta)\cos(2k\eta)\,d\eta, \\ N_k &= \int_0^{2\pi} \big[\bar{c}_0\big[\cosh(2\xi_0) + \cos(2\eta) + 2g(\eta, l)\sinh(2\eta_0)\big] + \Psi(\eta, l)\big]\cos(2k\eta)\,d\eta, \\ O_{k,m}^n &= \int_0^{2\pi} G(\eta, l)\operatorname{ce}_{2m}(\eta, -is_n)\operatorname{ce}_{2k}(\eta, -is_n)\,d\eta, \\ P_k^n &= \int_0^{2\pi} \bar{c}_n \operatorname{ce}_{2k}(\eta, -is_n)\,d\eta, \end{aligned}$$

with

$$\begin{aligned} \Psi(\eta, l) &= \varepsilon E\zeta\mu^{-1} + g(\eta, l)\psi'(\xi_0, \eta), \\ G(\eta, l) &= \operatorname{Ce}_{2m}(\xi_0, -is_n) + g(\eta, l)\operatorname{Ce}'_{2m}(\xi_0, -is_n). \end{aligned}$$

Equations (19) represent the infinite system of linear equations which can be used to compute the approximate values of A_{2m} and B_{2m}^n by reducing it to a system with finite terms of n, m and k, *i.e.*, $n = 0, 1, 2, \ldots, N$; $m = 0, 1, 2 \ldots, M$ and $k = 0, 1, 2, \ldots, K$ for suitable fixed positive numbers N, M, and K.

The solutions U_n, until now, contain the unknown potential ψ. In order to find $\psi(\xi, \eta)$, we assume that the influence of the convection is negligible and the electrolyte is symmetric. Hence, the ionic charge density can be expressed using the Boltzmann distribution of the number density of positive and negative ions as

$$p_e = ez_\nu(n_+ - n_-) = ez_\nu n_0 \sinh\left(\frac{ez_\nu\psi}{k_B T}\right), \tag{20}$$

where $n_\pm$ is the number density of the positive and negative ions, ε is the permittivity of the fluid, n_0 is the ionic concentration at the bulk, e is the elementary charge of a proton, z_ν is the valence of ions, k_B is the Boltzmann constant, and T is the fluid temperature.

Combining equations (7) and (20), we calculate ψ through the Poisson-Boltzmann equation

$$\nabla^2\psi(\xi,\eta) = -\frac{\rho_e}{\varepsilon} = \frac{2n_0 ez_v}{\varepsilon}\sinh\left(\frac{ez_v\psi}{k_BT}\right). \tag{21}$$

In the case of a low value of zeta potential, the Poisson-Boltzmann equation (21) is reduced to the Debye-Hückel approximation

$$\frac{1}{c^2(\cosh^2\xi - \cos^2\eta)}\left(\frac{\partial^2\psi}{\partial\xi^2} + \frac{\partial^2\psi}{\partial\eta^2}\right) - \kappa^2\psi = 0, \tag{22}$$

where $\kappa = (2n_0ez_v^2/k_BT)^{1/2}$ is the reciprocal of the EDL thickness. As in the case of W_n, the potential ψ in equation (22) can be obtained in a similar way. Using the boundary conditions (11a)-(11c) and (11e), we then have

$$\psi(\xi,\eta) = \sum_{m=0}^{\infty} D_m \operatorname{Ce}_{2m}(\xi;-q)\operatorname{ce}_{2m}(\eta;-q),$$

where $q = \kappa^2c^2/4$ and

$$D_m = \frac{\int_0^{2\pi}\zeta\cdot\operatorname{ce}_{2m}(\eta,-q)\,d\eta}{\int_0^{2\pi}\operatorname{Ce}_{2m}(\xi_0,-q)\operatorname{ce}_{2m}^2(\eta,-q)\,d\eta}.$$

As the fluid velocity is now known, the volumetric flow rate can be calculated through the formula

$$Q(t) = \int_0^{2\pi}\int_0^{\xi_0} c^2\left(\cosh^2\xi - \cos^2\eta\right)u(\xi,\eta,t)\,d\xi\,d\eta.$$

According to this formula, the numerical results of volumetric flow rate will be presented in the next section.

5 Numerical results and discussions

In this section, we show some numerical results of velocity profile under the oscillating pressure gradient and the electrokinetic force through an elliptical cylindrical channel at various times during a wave cycle. The presented results are achieved using the formula in equation (15) where the coefficients A_{2m}, B_{2m}^n are defined by equation (18) for the no-slip condition ($l = 0$) and equation (19) with the appropriate numbers $M = K = 6$ for the slip condition ($l > 0$). The solution in equation (15) is more general than the one in [7]; in other words, when the external electric field is zero and the pressure gradient does not oscillate ($dp/dz = c_0$), our solution reduces to

$$u(\xi,\eta) = \frac{A_0}{2} + \sum_{m=1}^{\infty} A_{2m}\cosh(2m\xi)\cos(2m\eta) + \bar{c}_0\left[\cosh(2\xi) + \cos(2\eta)\right]$$

which is exactly the one presented in [7].

The comparative results of volumetric flow rate on various numbers of the Fourier expansion terms, $N + 1$, for the pressure gradient defined in equation (10) and on various

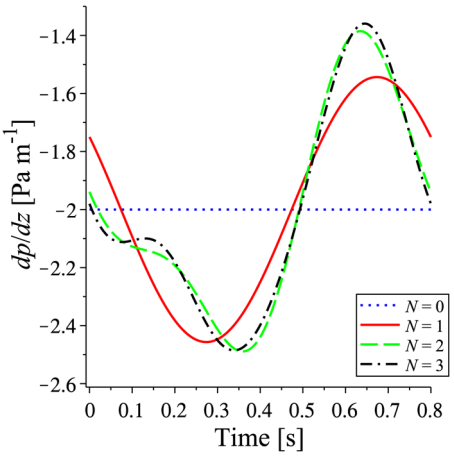

Figure 1 Four pressure gradient waveforms $dp/dz = \mathrm{Re}\left(\sum_{n=0}^{\infty} c_n e^{in\omega t}\right)$ **when** $N = 0$ **(dotted line),** $N = 1$ **(solid line),** $N = 2$ **(dashed line), and** $N = 3$ **(dash-dotted line).**

slip lengths l are presented. Moreover, an influence of oscillating term in a pressure gradient expression on electroosmotic flows with various external electric fields are investigated.

In this section, we use the fluid properties as appeared in Li's work [11]. The fluid is aqueous KCl solution (1:1 electrolyte) with the properties prescribed in parameters as follows: $\rho = 1.00 \times 10^3\ \mathrm{kg\,m^3}$; $\mu = 0.90 \times 10^{-3}\ \mathrm{kg\,m^{-1}\,s^{-1}}$; $\varepsilon = 6.95 \times 10^{-10}\ \mathrm{C\,V^{-1}\,m^{-1}}$; $\zeta = 2.49 \times 10^{-2}\ \mathrm{V}$; and $\kappa = 4 \times 10^4\ \mathrm{m^{-1}}$. The channel is the rigid tube of elliptic cross-section having the focus length $c = 90\ \mu\mathrm{m}$ and the eccentricity $\bar{e} = 0.60$. The waveform of pressure gradient as shown in Figure 1 is determined by setting the parameters $c_0 = -2$, $c_1 = 0.25 + 0.38i$, $c_2 = -0.19 + 0.03i$, $c_3 = -0.04 + 0.01i$, and $\omega = 2\pi(0.8)^{-1}$. Since the electroosmotic force in this study is considered to be positive, the negative pressure gradient force will reinforce the electroosmotic flow.

As the velocity u in equation (15) does not depend on z, the velocity profiles of mixed electroosmotic pressure-driven flow through the elliptical cylindrical channel are projected to the elliptic cross-section presented in Figure 2. The results are plotted using $N = 3$, $l = 1\ \mu\mathrm{m}$, and $E = 500\ \mathrm{V\,m^{-1}}$ at nine different times $t = 0, 0.15, 0.35, 0.45, 0.5, 0.55, 0.65, 0.75,$ and 0.8 s. The result shows the relation of flow to an oscillatory pressure gradient. The graph of velocity represents the forward flow with speed of $17.5\ \mu\mathrm{m\,s^{-1}}$ as a result of the positive electrokinetic force combined with the positive pressure force (negative pressure gradient). For $0.15 \leq t \leq 0.35$ s, the amplitude of the (negative) pressure gradient increases as time increases. This results in the increased pressure force, which causes an increase in the flow speed. At $t = 0.35$ s, as the (negative) pressure gradient decreases to the nadir (maximum amplitude), the forward speed reaches $20\ \mu\mathrm{m\,s^{-1}}$. For $0.45 \leq t \leq 0.65$ s, the amplitude of the (negative) pressure gradient decreases as time increases. This means that the pressure force decreases. As a result, the velocity combined with the pressure force drops. At $t = 0.65$ s, the velocity reduces to $15\ \mu\mathrm{m\,s^{-1}}$ because the (negative) pressure gradient increases to the peak (minimum amplitude). For $0.75 \leq t \leq 0.8$ s, the velocity increases as the amplitude of pressure gradient increases. At $t = 0.8$ s, the end of pressure gradient wave, the velocity profile is similar to the one at $t = 0$ s.

Figure 3 shows the variation in the ratio of volumetric flow rates corresponding to the oscillatory pressure gradient Q_{pp} and the constant one Q_{cp} with various external electric fields $E = 0, 500, 1{,}000,$ and $5{,}000\ \mathrm{V\,m^{-1}}$ using $l = 1\ \mu\mathrm{m}$. An expression based on 1-term

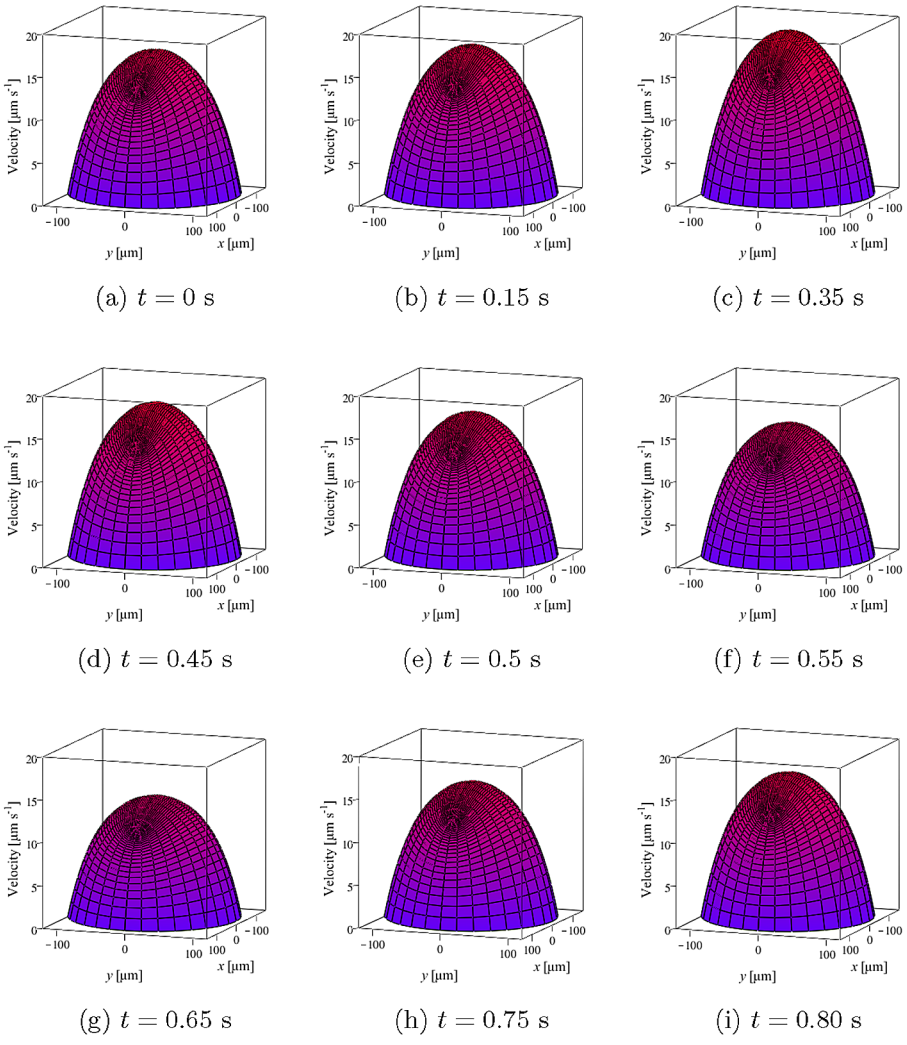

Figure 2 Velocity profiles with various times t = 0, 0.15, 0.35, 0.45, 0.5, 0.55, 0.65, 0.75, and 0.8 s for l = 1 μm, and E = 500 V m^{-1}.

and 4-term of the Fourier expansion for the pressure gradient ($N = 0$ and $N = 3$) is used in the case of Q_{cp} and Q_{pp}, respectively. It can be seen that the ratio Q_{pp}/Q_{cp} is in a wave form and its amplitude decreases with an increase of E from 0 to 1,000 V m^{-1}; when E = 5,000 V m^{-1}, the ratio Q_{pp}/Q_{cp} tends to a constant at 1. This physically means that, for $E = 0$, the flow is driven only by the pressure force. In this case, the result shows an extreme difference of the volumetric flow rate with and without considering the oscillating term of the pressure gradient. For $500 \leq E \leq 1{,}000$ V m^{-1}, the flow is driven by both the pressure gradient and the electroosmotic force. In this case, the effect of the oscillating term still significantly affects the volumetric flow rate. For E = 5,000 V m^{-1}, the electroosmotic force becomes dominant. In this case, there is a slight difference between the flow rates Q_{pp} and Q_{cp}. As a consequence, the pressure gradient force is practically negligible when E is very high. This investigation indicates an influence of the pulsatile pressure gradient on the electroosmotic flow rate with various external electric fields. The result shows that the oscillatory pressure gradient plays a crucial role in the control of the flow

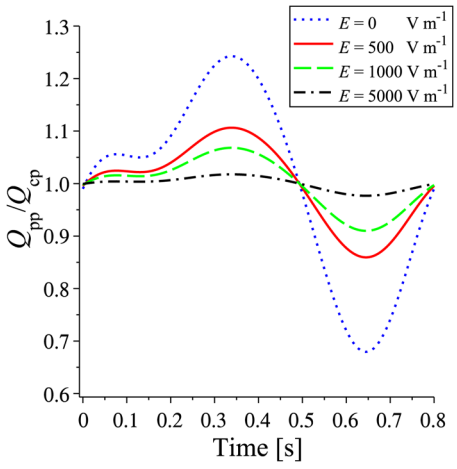

Figure 3 Variation in the ratio of volumetric flow rate corresponding to the oscillatory pressure gradient Q_{pp} and the constant one Q_{cp} with various external electric fields $E = 0, 500, 1{,}000,$ and $5{,}000\ \mathrm{V\,m^{-1}}$ for $N = 3$ and $l = 1\ \mu$m.

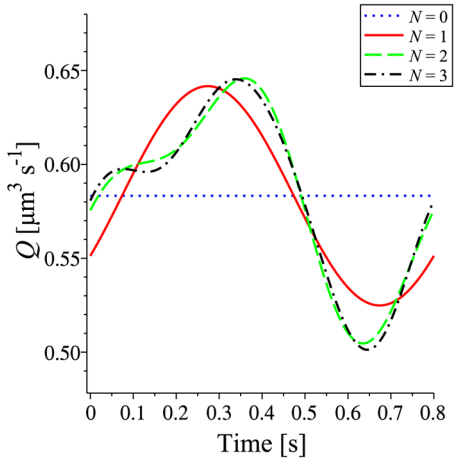

Figure 4 Variation of volumetric flow rate with various numbers of the Fourier expansion terms of the pressure gradient using $N = 0, 1, 2,$ and 3 for $l = 1\ \mu$m and $E = 500\ \mathrm{V\,m^{-1}}$.

in the microchannel of elliptic cross-section when the flow is evidently driven by both the pulsatile pressure gradient and the electrokinetic force.

Figure 4 shows the variation of volumetric flow rate corresponding to various numbers of the Fourier expansion terms of the pressure gradient using $N = 0, 1, 2,$ and 3 for $l = 1\ \mu$m and $E = 500\ \mathrm{V\,m^{-1}}$. It can be seen that the flow rate has a constant value of $0.58\ \mu\mathrm{m^3\,s^{-1}}$ when $N = 0$ (constant pressure gradient). The reasons for this occurrence are that the interpolation using only the first term of the Fourier series for the pulsatile pressure gradient represents just the mean pressure gradient, and the electroosmotic force is a constant. When $N \geq 1$, our results, related to the oscillation of the pressure gradient, develop traveling wave of fluid flow. For $N = 1$, the flow rate is in a sinusoidal form as a result of the sinusoidal interpolation of the pressure gradient. In the cases of $N = 2$ and 3, the flow rates appear to be similar and much closer together, but different from the flow rate when $N = 1$. This investigation indicates the significance of using the higher Fourier expansion term for pressure gradient to manipulate the flow rate. However, when a pressure gradient is approximated well enough, the numerical result of flow rate is precise and reliable.

Regarding the appearance of fluid slip in a microchannel, the variation of volumetric flow rate with various slip lengths $l = 0, 1, 2, 3, 4,$ and $5\ \mu$m is presented in Figure 5 using

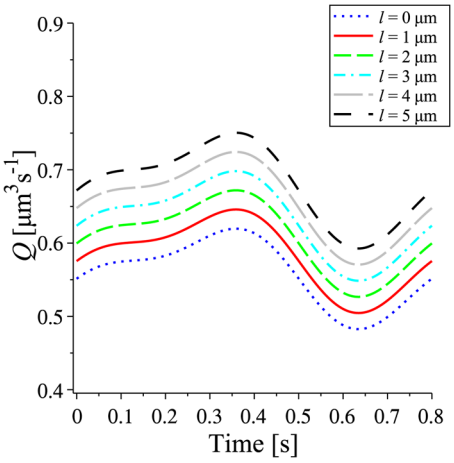

Figure 5 Variation of volumetric flow rate with various slip lengths $l = 0, 1, 2, 3, 4,$ and 5 μm for $N = 3$ and $E = 500\ \mathrm{V\,m^{-1}}$.

4-terms Fourier expansion ($N = 3$) of the pressure gradient and $E = 500\ \mathrm{V\,m^{-1}}$. The result shows that, for the particular value of the flow parameters used in this section, the volumetric flow rate with 1 μm slip length increases compared with the no-slip flow rate. This result is consistent with the experiment in [16] and the numerical result obtained from the analytical solution of a circular microchannel [6]. In fact, both claimed results imply that the velocity increases on the entire velocity profile when the slip condition is taken into consideration. A velocity increase will directly result in an increase in the flow rate. However, it can be seen that the flow rate of $l = 1$ μm is only 5% difference in value compared to the one of no-slip condition. It may be concluded that when the slip length is less than 1 μm, the slip condition can be omitted to reduce the computational cost. Figure 5 also shows that the flow rate gradually increases as the slip length increases. The flow rate increases to approximately 10%, 15%, 20%, and 25% higher when $l = 2, 3, 4,$ and 5 μm, respectively. This result agrees well with the one obtained in [25], which presents the velocity shift constantly upwards as the slip length increases. For the flow with higher slip length, the slip condition should be considered in the mathematical model to bring a more accurate result.

6 Conclusions

The primary objectives of the present work were twofold. One was to find the solution of an unsteady pulsatile pressure-driven electroosmotic flow through an elliptic cylindrical microchannel with the Navier slip condition. The solution was solved with the use of the Mathieu and modified Mathieu functions. The other was to investigate our numerical results to develop a better understanding of the underlying physical processes in microfluidics. In particular, we compared the volumetric flow rate corresponding to the oscillatory and the constant pressure gradient, the volumetric flow rate with the number of the Fourier expansion terms for the pressure gradient, and the volumetric flow rate with the slip length. We found that when the flow was clearly driven by a combination of pressure and electrokinetic forces, the oscillatory behavior of pulsatile pressure became crucial especially when external electric field was low. The volumetric flow rate is more accurate as we use a higher number of terms in the Fourier expansion for pressure gradient. Moreover, an increment in slip lengths gives rise to an increment in volumetric flow rate in a proportional way.

Competing interests
The authors declare that they have no competing interests.

Authors' contributions
All authors read and approved the final manuscript.

Author details
[1]Department of Mathematics, Faculty of Science, Mahidol University, Rama VI Road, Bangkok, 10400, Thailand. [2]The Centre of Excellence in Mathematics, Si Ayutthaya Road, Bangkok 10400, Thailand. [3]Department of Mathematics and Statistics, Faculty of Science and Engineering, Curtin University, Perth, WA, Australia.

Acknowledgements
This work is partially supported by Development and Promotion of Science and Technology Talents Project (DPST).

Publisher's Note

Received: 31 January 2017 Accepted: 17 May 2017 Published online: 07 June 2017

References

1. Gad-el-Hak, M: The fluid mechanics of microdevices - the Freeman scholar lecture. J. Fluids Eng. **121**(1), 5-33 (1999)
2. Beskok, A, Korniadakis, GE: Report: a model for flows in channels, pipes, and ducts at micro and nano scales. Microscale Thermophys. Eng. **3**(1), 43-77 (1999)
3. Araki, T, Kim, MS, Suzuki, K: An experimental investigation of gaseous flow characteristics in microchannels. Microscale Thermophys. Eng. **6**(2), 117-130 (2002)
4. Saidi, F: Non-Newtonian flow in a thin film with boundary conditions of Coulomb's type. Z. Angew. Math. Mech. **86**(9), 702-721 (2006)
5. You, D, Moin, P: Effects of hydrophobic surfaces on the drag and lift of a circular cylinder. Phys. Fluids **19**(8), 081701 (2007)
6. Yang, J, Kwok, DY: Microfluid flow in circular microchannel with electrokinetic effects and Navier's slip condition. Langmuir **19**(4), 1047-1053 (2003)
7. Duan, Z, Muzychka, YS: Slip flow in elliptic microchannels. Int. J. Therm. Sci. **46**, 1104-1111 (2007)
8. Duan, Z: Slip flow in doubly connected microchannels. Int. J. Therm. Sci. **58**, 45-51 (2012)
9. Lee, HB, Yeo, IW, Lee, KK: Water flow and slip on NAPL-wetted surfaces of a parallel-walled fracture. Geophys. Res. Lett. **34**(19), L19401 (2007)
10. Goswami, P, Chakraborty, S: Semi-analytical solutions for electroosmotic flows with interfacial slip in microchannels of complex cross-sectional shapes. Microfluid. Nanofluid. **11**(3), 255-267 (2011)
11. Li, D: Electrokinetics in Microfluidics. Elsevier, Amsterdam (2004)
12. Goldstein, D, Handler, R, Sirovich, L: Modeling a no-slip flow boundary with an external force field. J. Comput. Phys. **105**(2), 354-366 (1993)
13. Feng, ZG, Michaelides, EE: Robust treatment of no-slip boundary condition and velocity updating for the lattice-Boltzmann simulation of particulate flows. Comput. Fluids **27**(2), 370-381 (2009)
14. Bolintineanu, DS, Lechman, JB, Plimpton, SJ, Grest, GS: No-slip boundary conditions and forced flow in multiparticle collision dynamics. Phys. Rev. E, Stat. Nonlinear Soft Matter Phys. **86**(6), 066703 (2012)
15. Cohen, Y, Metzner, AB: Apparent slip flow of polymer solutions. J. Rheol. **29**(1), 67-102 (1985)
16. Tretheway, DC, Meinhart, CD: Apparent fluid slip at hydrophobic microchannel walls. Phys. Fluids **14**(3), 9-12 (2002)
17. Choi, CH, Westin, WJA, Breuer, KS: Apparent slip flows in hydrophilic and hydrophobic microchannels. Phys. Fluids **15**(10), 2897-2902 (2003)
18. Na, R, Jian, Y, Chang, L, Su, J, Liu, Q: Transient electro-osmotic and pressure driven flows through a microannulus. Open J. Fluid Dyn. **3**(2), 50-56 (2013)
19. Chinyoka, T, Makinde, OD: Analysis of non-Newtonian flow with reacting species in a channel filled with a saturated porous medium. J. Pet. Sci. Eng. **121**, 1-8 (2014)
20. Reshadi, M, Saidi, MH, Firoozabadi, B, Saidi, MS: Electrokinetic and aspect ratio effects on secondary flow of viscoelastic fluids in rectangular microchannels. Microfluid. Nanofluid. **20**, 117 (2016)
21. Bandopadhyay, A, Chakraborty, S: Electrokinetically induced alterations in dynamic response of viscoelastic fluids in narrow confinements. Phys. Rev. E **85**, 056302 (2012)
22. Chakraborty, J, Ray, S, Chakraborty, S: Role of steaming potential on pulsating mass flow rate control in combined electroosmotic and pressure-driven microfluidic devices. Electrophoresis **33**, 419-425 (2012)
23. Mathieu, EL: Mémoire sur le mouvement vibratoire d'une membrane de forme elliptique. J. Math. Pures Appl. **13**, 137-203 (1868)
24. Mclachlan, NW: Theory and Application of Mathieu Functions. Clarendon, Oxford (1947)
25. Salehi, GR, JalaliBidgoli, M, ZeinaliDanaloo, S, HasanZadeh, K: An investigation on micro slip flows in micro channels. In: Proceedings of the ASME 2010 10th Biennial Conference on Engineering Systems Design and Analysis, ESDA2010, vol. 5, pp. 517-523 (2010)